IFM - 15 / 92

Initial-final state interference in $e^+e^- \to H\mu^+\mu^-$

P. Nogueira and J. C. Romão
CFMC, Av. Prof. Gama Pinto 2, P-1699 Lisboa Codex, Portugal

Abstract

Here we take the process $e^+e^- \to H\mu^+\mu^-$ and compute a special class of one-loop QED corrections, namely the interference effects between the initial and final state radiation (interference radiation for short). This analysis is restricted to soft bremsstrahlung.

December 1992

1 Introduction

The evaluation of radiative corrections is a crucial task for all accurate measurements of particle physics. At present accelerator energies the usually dominant radiative corrections are the QED corrections. In this paper we check the magnitude of the interference radiation on the five body process $e^+e^- \to H\mu^+\mu^-$, for which we compute the initial-final state interference radiation at 1-loop. For processes of this kind the one-loop QED corrections may be divided into three groups, every group being finite and gauge invariant. Specifically, one has corrections due to initial state radiation, final state radiation, and their interference. Generally, the initial state radiation is expected to dominate.

The process $e^+e^- \to H\mu^+\mu^-$ is regarded as a clean possibility for the Higgs boson detection and has already received much attention. The evaluation of the initial-state radiation was done by Berends and Kleiss [1]. Fleischer e Jegerlehner computed both QED and weak corrections [2,3], although using an on-shell approximation for the Z decaying in the muon pair. This amounts to decompose the original process into a chain reaction: first $e^+e^- \to HZ$ and then $Z \to \mu^+\mu^-$. In this way there are no 5-point functions to evaluate, but then the interference radiation is simply ignored.

To the best of our knowledge, a single example exists in the literature where the role of the 5-point function in $O(\alpha)$ QED corrections was analyzed [4]. In that case the corrections were found to be extremely small. The process here studied has quite different features. Instead of a two photon process one has an e^+e^- annihilation reaction; instead of QED the underlying model is the GWS Model where, for example, gauge boson couplings to fermions are not just vectorial; instead of a process where (at tree level) the vanishing photon mass is probably the most important feature we now have a process where the width of an unstable particle plays a major role.

This paper is organized as follows. In section 2 we present both virtual and bremsstrahlung corrections, and check the cancelation of infrared divergences. Section 3 contains a short discussion on the numerical evaluation and Z-width effects. Our main results are described in section 4. The appendix contains general expressions for the form factors of some 5-point integrals.

2 The initial-final state interference corrections

If one neglects the Yukawa couplings for both the electron and the muon then a single tree level diagram is left for the process $e^+(p_2)\,e^-(p_1) \to H(p_H)\,\mu^+(p_4)\,\mu^-(p_3)$, which is depicted in figure 1 (top). For convenience we define the following kinematical variables.

$$s = (p_1 + p_2)^2$$
$$\bar{s} = (p_3 + p_4)^2 \qquad (1)$$

Let us expand both the Lorentz invariant amplitude $\mathcal{M}$ and the differential cross section $d\sigma$ in the number of loops:

$$\mathcal{M} = \mathcal{M}_0 + \mathcal{M}_1 + \mathcal{M}_2 + \ldots \qquad (2)$$
$$d\sigma = d\sigma_0 + d\sigma_1 + d\sigma_2 + \ldots \qquad (3)$$

Then the $O(\alpha)$ correction to the differential cross section may be written as

$$d\sigma_1 = \frac{(2\pi)^4}{4\sqrt{(p_1\cdot p_2)^2 - m_e^4}} \cdot \frac{1}{4}\sum_{pol}\left\{2Re\left(\mathcal{M}_0^\dagger \mathcal{M}_1\right) + C_{sb}\,|\mathcal{M}_0|^2\right\} d\Phi_3 \, . \qquad (4)$$

Here the integration is done over the 3-body Lorentz invariant phase space and the sum is performed over all the polarization states, both initial and final. The soft bremsstrahlung contribution has been added in order to make the cross section finite. As it is well known, this term factorizes into the tree level cross section $d\sigma_0$ and the Bremsstrahlung integral C_{sb} if the soft photon approximation is used.

As we seek to evaluate the class of corrections $d\sigma_{int}$ that come from the interference radiation, we keep only a subset of the contributions displayed in equation 4. For the amplitude $\mathcal{M}_1$ only the 1-loop diagrams depicted in figure 1 are taken into account. Omitting polarization indices we write it as a sum of four amplitudes, one for each diagram (note that T_4 is written explicitely in expression 7):

$$\mathcal{M}_1 \leftarrow T_1 + T_2 + T_3 + T_4 \qquad (5)$$

The bremsstrahlung integral, that may be computed from the diagrams drawn in figure 2, reduces to

$$C_{sb} = -\frac{e^2}{(2\pi)^3}\int_{|\mathbf{k}|\le\omega} \frac{d^3k}{2k^0}\left(\frac{2p_1\cdot p_4}{(k\cdot p_1)(k\cdot p_4)} - \frac{2p_1\cdot p_3}{(k\cdot p_1)(k\cdot p_3)} + \frac{2p_2\cdot p_3}{(k\cdot p_2)(k\cdot p_3)} - \frac{2p_2\cdot p_4}{(k\cdot p_2)(k\cdot p_4)}\right) . \qquad (6)$$

Both the virtual and soft photon corrections are infrared divergent; in the following we check that their sum is well behaved, as it should be expected. The virtual corrections include the *four* pentagons displayed in figure 1, while the bremsstrahlung contribution (equation 6) consists of *four* crossed terms. In every 1-loop diagram the photon connects an incident fermion to an outgoing fermion. Every bremsstrahlung term depends only on two fermion momenta, one from the initial state and the other from the final state. Moreover, all four possibilities are present in both cases. This defines a natural association between the pentagons and the bremsstrahlung terms. Due to the absence of renormalization artifacts (that may afflict fermion self-energies or vertex corrections, for instance) the cancelation of infrared divergencies is clear: the sum of the contributions coming from each pair { pentagon, bremsstrahlung term } is infrared finite.

For example let us take the pentagon where the photon is incident with the positron and the negatively charged muon. The amplitude for such diagram is given by

$$T_4 = \frac{e^5 m_Z}{8\pi^2 \sin^3 2\theta_W} \int \frac{d^4k}{i\pi^2} \frac{1}{k^2 - m_\gamma^2 + i\varepsilon} \cdot \frac{1}{(k+p_2)^2 - m_e^2 + i\varepsilon}$$

$$\cdot \frac{1}{(k+p_1+p_2)^2 - m_Z^2 + i\varepsilon} \cdot \frac{1}{(k+p_4+p_3)^2 - m_Z^2 + i\varepsilon} \cdot \frac{1}{(k+p_3)^2 - m_\mu^2 + i\varepsilon}$$

$$\cdot \bar{v}(p_2)\, \gamma_\mu \left(- \not{k} - \not{p}_2 + m_e\right) \gamma_\alpha \left(g_V - g_A \gamma_5\right) u(p_1)$$

$$\cdot\, \bar{u}(p_3)\, \gamma^\mu \left(\not{k} + \not{p}_3 + m_\mu\right) \gamma^\alpha \left(g_V - g_A\gamma_5\right) v(p_4) \qquad (7)$$

where we have ignored polarization indices. The Z coupling to charged leptons is denoted by

$$\frac{ie}{\sin 2\theta_W} \gamma^\alpha \left(g_V - g_A\gamma_5\right) \qquad (8)$$

$$g_A = \tfrac{1}{2}\,, \quad g_V = -\frac{1}{2} + 2\sin^2\theta_W$$

As we happen to be interested in the infrared divergence, we may set k to zero in the numerator of expression 7. Thus

$$T_4^{IR} \sim -\frac{e^2}{4\pi^2} (p_2 \cdot p_3)\, \mathcal{M}_0 C_0^{IR} \qquad (9)$$

and

$$2Re\left(\mathcal{M}_0^\dagger T_4^{IR}\right) \sim -\frac{e^2}{2\pi^2} (p_2 \cdot p_3) \left|\mathcal{M}_0\right|^2 Re\left(C_0^{IR}\right) \qquad (10)$$

The symbol $\sim$ denotes similar infrared behaviour and C_0^{IR} stands for the infrared divergent integral

$$C_0^{IR} = \int \frac{d^4k}{i\pi^2} \frac{1}{k^2 - m_\gamma^2 + i\varepsilon} \cdot \frac{1}{(k+p_2)^2 - m_e^2 + i\varepsilon} \cdot \frac{1}{(k-p_3)^2 - m_\mu^2 + i\varepsilon}\,. \qquad (11)$$

On the other hand the contribution from the corresponding soft bremsstrahlung term is

$$-\frac{e^2}{8\pi^3} \left|\mathcal{M}_0\right|^2 \int \frac{d^3k}{2k^0} \frac{2p_2 \cdot p_3}{(p_2 \cdot k)(p_3 \cdot k)} \qquad (12)$$

It is a simple matter to verify that the sum of these expressions is infrared finite. Equation 10 has the following divergent behaviour

$$-\frac{e^2}{4\pi^2} \left|\mathcal{M}_0\right|^2 \frac{\xi}{\sqrt{\xi^2 - 1}} \log\left(\xi + \sqrt{\xi^2 - 1}\right)^2 \cdot \log m_\gamma \qquad (13)$$

which is exactly canceled by expression 12. Here ξ denotes

$$\frac{p_2 \cdot p_3}{m_e m_\mu} \qquad (14)$$

The same kind of cancelation occurs for every other pair.

3 Numerical evaluation and Z-width effects

The Z boson width plays a major role in this process. In the kinematical region under study ($\sqrt{s} > m_H + m_Z$), the amplitude is completely regulated by Γ_Z since it becomes infinite for $\Gamma_Z = 0$. This occurs not only at tree level but also at higher orders. After reducing the various five-point functions to scalar 3- and 4-point integrals this divergence appears in some of the latter integrals. This is why some boxes and triangles must be evaluated with a nonzero width Γ_Z (here we mean replacing $-m_Z^2 + i\varepsilon$ by $-m_Z^2 + i m_Z \Gamma_Z$ in the Z propagators).

In the first place the reduction of the one-loop amplitude was performed using the form factor decomposition presented in equations A.10 and A.11 (see appendix). For the evaluation of the scalar 3-point functions (figure 4) the package **ff** [5] was used, for either real or complex masses. In the case of the scalar four-point integrals no package is (at present) general enough. We split the five kinds of boxes into three groups (figure 3). The boxes in the top row are infrared divergent and may be evaluated using the results of reference [6], even for complex m_Z. The box in the middle was evaluated numerically by the **ff** routines neglecting the Z-width, since this box is regular in that approximation; the possibility of including the Z-width might be available soon [7] but we do not expect this approximation to change our main conclusions.

Finally there are the two boxes in the lower row; even assuming that $\sqrt{s} > m_Z$ these boxes are infrared singular whenever $\sqrt{\bar{s}} = m_Z$, that is, deep inside the region of the dominant kinematical configuration. An exact expression for these boxes has been constructed, and we were able to show that analytic continuation in m_Z was simple provided that $\sqrt{s} > m_H + \sqrt{\bar{s}}$ and for Γ_Z not too large (for example, $\Gamma_Z \leq m_Z$ has no problem). In our case these conditions are trivially satisfied but the general solution for this kind of box seems harder to find.

4 Results

For the Z and W boson masses we took $m_Z = 91.17 GeV$ and $m_W = 80.0 GeV$, respectively (unless stated otherwise). Only the energy range $\sqrt{s} > m_Z + m_H$ is explored, since this is most likely the best place to look at this process; on the other hand the cross section is more slowly varying which is more suitable to apply the soft photon approximation.

The fine structure constant is defined in the low energy limit and the Weinberg angle is defined in terms of the vector boson masses:

$$\cos\theta_W = \frac{m_W}{m_Z} \qquad (15)$$

In principle the photon energy cut-off ω should be taken as the experimental resolution of the charged particles energy. In the absence of specific data we take $\omega = k_0 E_{min}$, that is, a fraction of the minimal muon-pair energy

$$E_{min} = \frac{s - m_H^2 + 4m_\mu^2}{2\sqrt{s}} \, . \qquad (16)$$

In almost every plot we take $k_0 = 0.1$; thus ω does not exceed 10% of the muon-pair energy (nor 10% of the beam energy). This should not be too far from reality and should be enough for the purpose of estimating the magnitude of the interference corrections.

The numerical integration was performed by the *RIWIAD* routine [8]. In figures 5 to 8 the ratio

$$R_{int} = \frac{\sigma_{int}}{\sigma_0} \qquad (17)$$

is plotted for different choices of the parameters. Figure 5 and 6 show this ratio for $m_H = 60 GeV$ and $m_H = 80 GeV$ respectively. These values are very small and, most likely, negative. A fairly strong cancelation between negative and positive contributions to σ_{int} seems to be at the origin of the large relative error. To obtain figure 7 we used the same input as for figure 5 except that k_0 is now 0.01; this shows that the particular value $k_0 = 0.1$ has little to do with the cancelation observed.

After obtaining these results we have made some effort to try to understand this unusual numerical cancelation. If instead of assuming a fixed value for m_W we allow it to take different values then one is inducing a varying $Zl\bar{l}$ coupling (through $\sin\theta_W$), thus affecting the cross section. In figure 8 R_{int} is plotted as a function of m_W, while the beam energy is kept constant. The cancelation seems fortuitous: corrections could be higher than 1% were m_W rather different from $80 GeV$. One can also observe that this cancellation seems maximal when $\sin\theta_W$ is close to 1/2 (then $m_W = 79 GeV$), that is, when the vectorial coupling for the vertex $Zl\bar{l}$ becomes zero.

To estimate how strong were these numerical cancelations we computed

$$\bar{R}_{int} = \frac{\int |d\sigma_{int}|}{\sigma_0} \, . \qquad (18)$$

For the same energy values as in figure 7 we obtained the fairly constant result $\bar{R}_{int} = 0.019$. This shows that even if the cancelations just discussed were absent the corrections could nt be much higher than 1%.

It is known that the introduction of mass widths might spoil the gauge invariance of the cross section perturbative expansion. This question has not yet been appropriately tackled. However, we tried to estimate its influence on the result by setting $\Gamma_Z = 0$ where possible and then comparing with the results previously obtained for $\Gamma_Z \neq 0$. This seemed to support the validity of our calculation, since no significant changes have been observed when the 1-loop corrections were of the order of 1%. For smaller values the accuracy of our calculations is not sufficient to rule out such a possibility; but then these values are just to small to justify further investigation.

Summarizing, due to an accidental cancelation the initial-final state interference radiation will be completely negligible for this particular process. Its evaluation might be required for other five-body processes should the experimental error be small enough (at least when it is at the level of 1% or better).

Acknowledgments

We would like to thank G. van Oldenborgh for providing us with his program **ff** at an early stage and for several related discussions.

References

[1] F. A. Berends and R. Kleiss. *Nucl. Phys.* *B*260, 32, 1985.

[2] J. Fleischer and F. Jegerlehner. *Nucl. Phys.* *B*216, 469, 1983.

[3] J. Fleischer and F. Jegerlehner. Preprint BI-TP 87/04. Fakultät für Physik, Universität Bielefeld.

[4] W. L. van Neerven and J. A. M. Vermaseren. *Phys. Lett.* *B*142, 80, 1984.

[5] G. J. van Oldenborgh. *Comp. Phys. Comm.* **66**, 1, 1991.

[6] W. Beenakker and A. Denner. *Nucl. Phys.* *B*338, 349, 1990.

[7] G. J. van Oldenborgh. Preprint LMU-92/01. Ludwig-Maximilians Universität.

[8] B. Lautrup. RIWIAD: CERN-DD Long Writeup D114. 1982.

[9] D. B. Melrose. *Il Nuovo Cimento* **60**, 181, 1965.

[10] W. L. van Neerven and J. A. M. Vermaseren. *Phys. Lett.* *B*137, 241, 1984.

[11] G. Passarino and M. Veltman. *Nucl. Phys.* *B*160, 151, 1979.

A Appendix

Five-point integrals and form factors

An equation for reducing the five-point scalar function (see figure 9)

$$E_0 = \int \frac{d^4k}{i\pi^2} \frac{1}{N_1 N_2 N_3 N_4 N_5}\,, \tag{A.1}$$

where

$$N_i \equiv \left(k + \sum_{j=1}^{i-1} p_i\right)^2 - m_i^2\,, \tag{A.2}$$

to a linear combination of four-point scalar functions is already known [9,10]. Here we give an alternative derivation, and then we list explicit formulas for reduction of some tensor functions to form factors (in the Passarino-Veltman scheme [11]).

The basic argument is the fact that in four dimensions any five vectors are linearly dependent. Let us assume that p_1, p_2, p_3, p_4 are linearly independent vectors; then, for any four-vector k, one may express k^2 in the following way

$$k^2 = \sum_{i,j=1}^{4} G^{-1}_{i,j} \,(p_i \cdot k)\,(p_j \cdot k) \tag{A.3}$$

where we have used the Gram matrix

$$G_{i,j} = p_i \cdot p_j\,, \quad i,j = 1,2,3,4 \tag{A.4}$$

Now use the relations

$$\begin{aligned} k^2 &= N_1 + m_1^2 \\ 2k \cdot p_i &= N_{i+1} - N_i + m_{i+1}^2 - m_i^2 - p_i^2 - 2\sum_{j=1}^{i-1} p_i \cdot p_j \\ &\equiv N_{i+1} - N_i + \eta_i\,, \quad \text{i=1,2,3,4} \end{aligned} \tag{A.5}$$

in equation A.3 to obtain

$$1 = \xi^{-1} \sum_{i=1}^{5} \alpha_i N_i + \xi^{-1} \sum_{i=1}^{5} (r_i \cdot k_i)\, N_i \tag{A.6}$$

Here we have defined

$$\begin{aligned} k_i^\mu &= k^\mu + \sum_{j=1}^{i} p_i^\mu \\ \alpha_i &= -2\delta_{i,1} + \sum_j \left(G^{-1}_{i-1,j} - G^{-1}_{i,j}\right) \eta_j \\ r_i^\mu &= 2\sum_j \left(G^{-1}_{i-1,j} - G^{-1}_{i,j}\right) p_j^\mu \\ \xi &= 4m_1^2 - \sum_{i,j=1}^{4} G^{-1}_{i,j} \eta_i \eta_j \end{aligned} \tag{A.7}$$

The quantities k_i^μ, r_i^μ and α_i are defined for $i = 1$ through 5. In the diagram of the 5-point integral it is possible to choose the pair (m_1, p_1) in 10 different ways. The quantity ξ is the same for any such choice, although this is not clear from the expression above.

It is not difficult to check that (after using identity A.6 in the numerator of the scalar five-point integrand) the contribution coming from the terms linear in k^μ vanish after integration in k-space, leaving us with an identity relating the scalar five-point integral in terms of scalar four-point integrals only:

$$E_0 = \xi^{-1} \sum_{j=1}^{5} \alpha_j D_0(j) \tag{A.8}$$

where

$$D_0(j) \equiv \int \frac{d^4k}{i\pi^2} \frac{N_j}{N_1 N_2 N_3 N_4 N_5} \tag{A.9}$$

In order to evaluate the one-loop amplitudes considered in this paper (e.g. equation 7), the reduction of vector and tensor integrals to scalar integrals is most convenient. Our notation for the five-point form factors is slightly different from the one used in ref. [11] for lower-point functions. We define

$$\int \frac{d^4k}{i\pi^2} \frac{k^\mu}{N_1 N_2 N_3 N_4 N_5} \equiv \sum_{i=1}^{4} E_i\, p_i^\mu \tag{A.10}$$

$$\int \frac{d^4k}{i\pi^2} \frac{k^\mu k^\nu}{N_1 N_2 N_3 N_4 N_5} \equiv \sum_{i,j=1}^{4} E_{i,j}\, p_i^\mu p_j^\nu \tag{A.11}$$

In this case no form factor in $g^{\mu\nu}$ is needed due to the identity

$$g^{\mu\nu} = \sum_{i,j=1}^{4} G^{-1}_{i,j} p_i^{\mu} p_j^{\nu} \tag{A.12}$$

The matrix $E_{i,j}$ is necessarily symmetric; a complete computation of its elements may serve as a simple check or even to estimate the accuracy of the numerical calculation.

The form factors just defined may be computed as follows.

$$E_i = \frac{1}{2}\sum_{j=1}^{4} G^{-1}_{i,j}\left(\eta_j E_0 + D_0(j+1) - D_0(j)\right) \tag{A.13}$$

$$E_{i,j} = \frac{1}{2}\sum_{k=1}^{4} G^{-1}_{i,k}\left(a_{k,j} + \eta_k E_j\right) \tag{A.14}$$

Here the quantities $a_{k,j}$ are implicitely defined by

$$\int \frac{d^4k}{i\pi^2}\, \frac{k^{\mu}\left(N_{k+1} - N_k\right)}{N_1 N_2 N_3 N_4 N_5} = \sum_{j=1}^{4} a_{k,j} p_j^{\mu} \;, \tag{A.15}$$

and may be further expressed in terms of scalar integrals.

B Figure Captions

Figure 1

Tree-level diagram for $e^+e^- \to H\mu^+\mu^-$ (top) and 1-loop QED diagrams for the initial-final state interference.

Figure 2

Tree-level diagrams for $e^+e^- \to H\mu^+\mu^-\gamma$ (bremsstrahlung diagrams).

Figure 3

Scalar 4-point integrals that appear in the reduction of the one-loop amplitude. Here (r_1, r_2) is a permutation of (p_1, p_2), and (r_3, r_4) is a permutation of (p_3, p_4).

Figure 4

Scalar 3-point integrals that appear in the reduction of the one-loop amplitude. Here (r_1, r_2) is a permutation of (p_1, p_2), and (r_3, r_4) is a permutation of (p_3, p_4).

Figure 5

Ratio R_{int} as a function of $\sqrt{s}$. Here $m_H = 60GeV$, $m_W = 80GeV$ and $k_0 = 0.1$; error bars correspond to a 90% confidence level.

Figure 6

Ratio R_{int} as a function of $\sqrt{s}$. Here $m_H = 80GeV$, $m_W = 80GeV$ and $k_0 = 0.1$; error bars correspond to a 90% confidence level.

Figure 7

Ratio R_{int} as a function of $\sqrt{s}$. Here $m_H = 60GeV$, $m_W = 80GeV$ and $k_0 = 0.01$; error bars correspond to a 90% confidence level.

Figure 8

Ratio R_{int} as a function of m_W. Here $m_H = 60GeV$, $\sqrt{s} = 180GeV$ and $k_0 = 0.1$; error bars correspond to a 90% confidence level.

Figure 9

Notation and diagrammatic representation for the scalar 5-point integral.

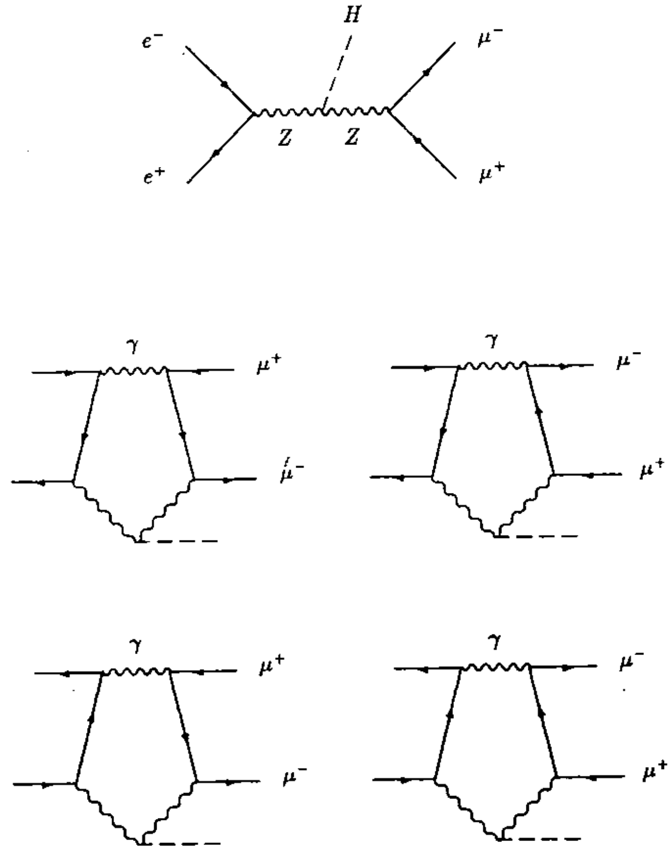

Figure 1

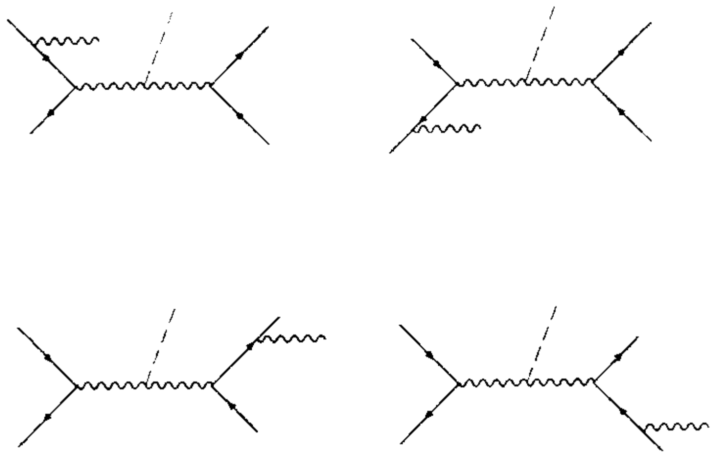

Figure 2

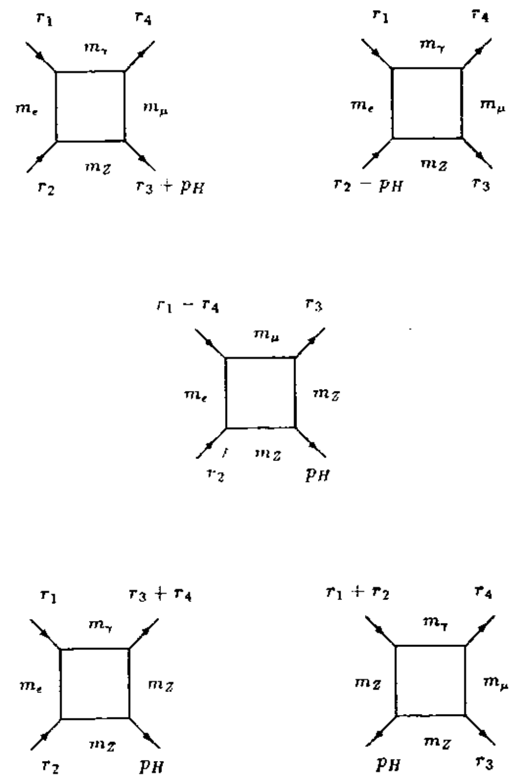

Figure 3

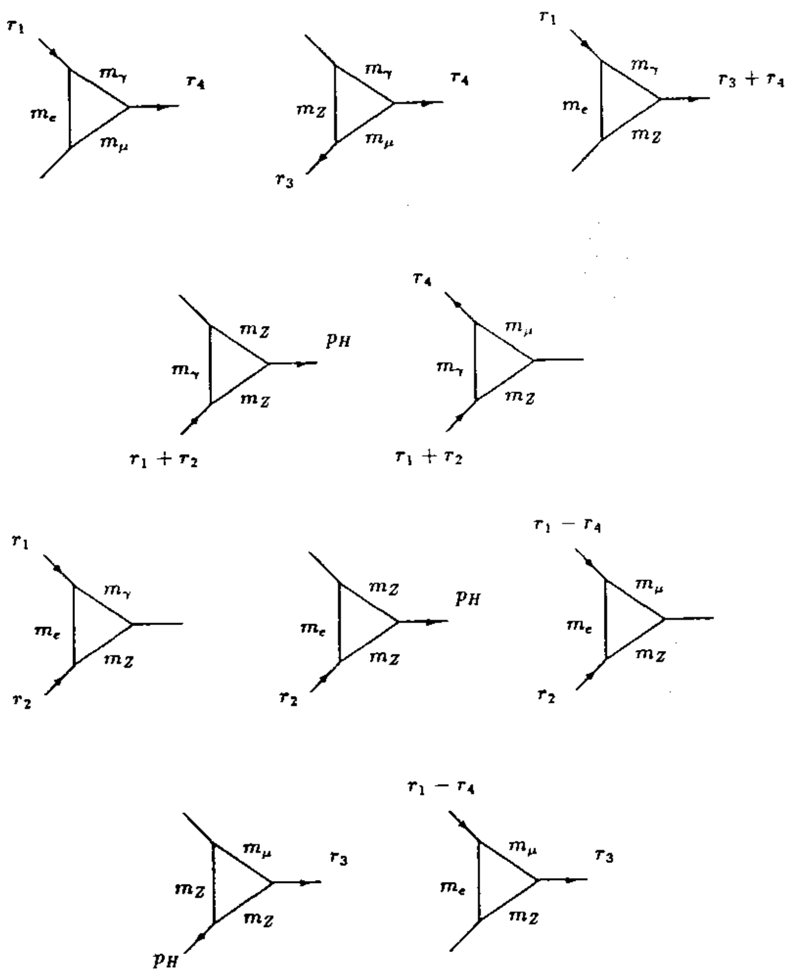

Figure 4

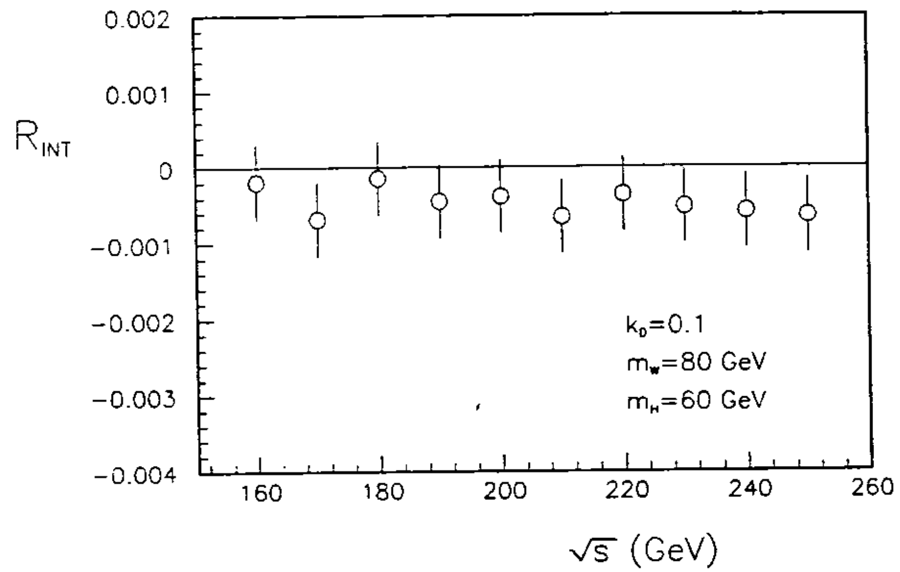

Figure 5

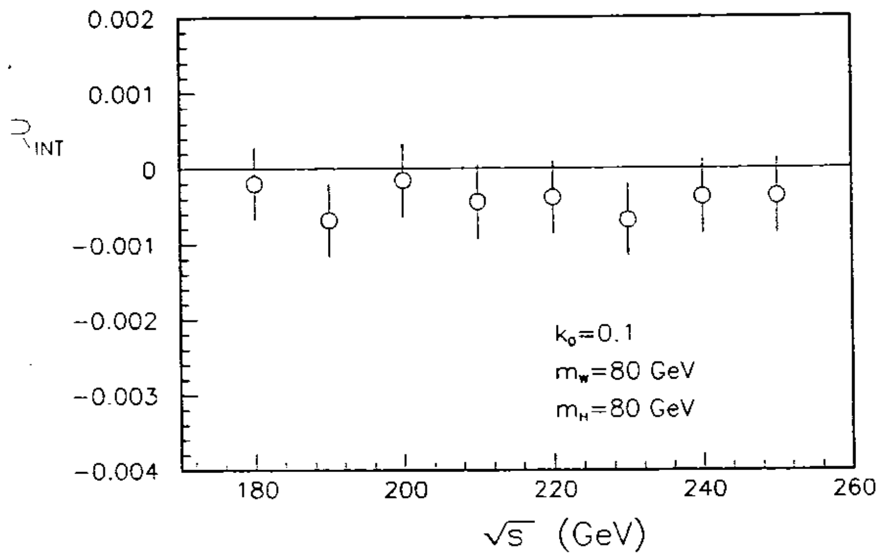

Figure 6

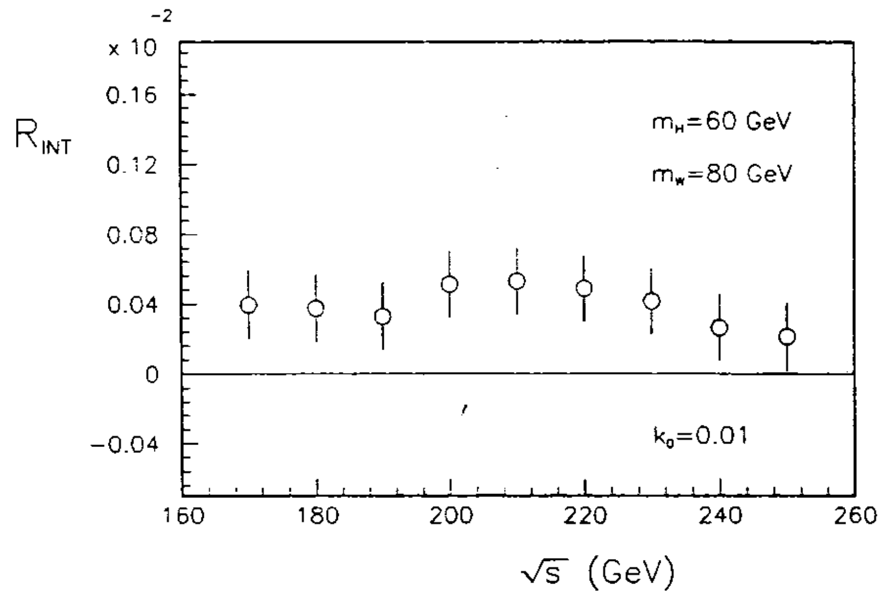

Figure 7

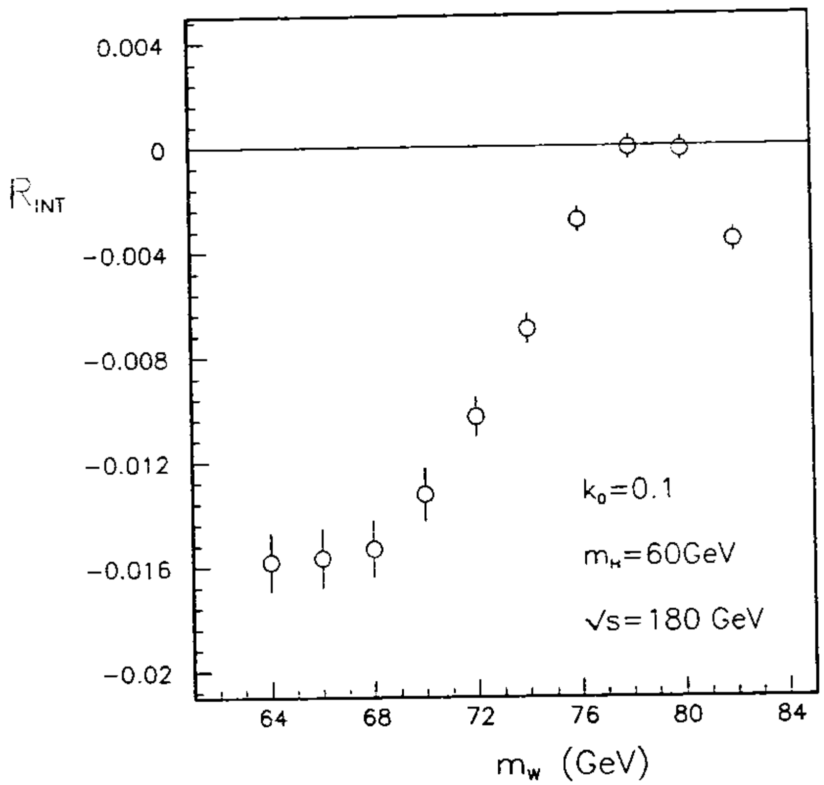

Figure 8

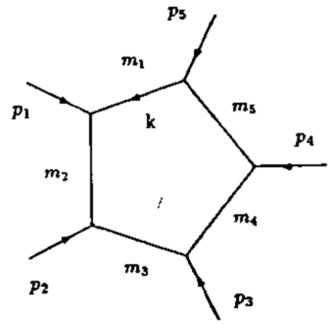

Figure 9